Hindawi
International Journal of Photoenergy
Volume 2018, Article ID 2769213, 8 pages
https://doi.org/10.1155/2018/2769213

Research Article

Mathematical Modeling and Mechanism of VUV Photodegradation of H_2S in the Absence of O_2

Jian-hui Xu,[1] Bin-bin Ding,[2] Xiao-mei Lv,[1] Shan-hong Lan,[1] Chao-lin Li,[2] and Liu Peng[1]

[1]*School of Environmental and Civil Engineering, Dongguan University of Technology, Dongguan, Guangdong 523808, China*
[2]*Environmental Science and Engineering Center, Harbin Institute of Technology Shenzhen Graduate School, Shenzhen, Guangdong 518055, China*

Correspondence should be addressed to Xiao-mei Lv; lvxiaomei.daisy@gmail.com

Received 7 February 2018; Revised 14 April 2018; Accepted 14 May 2018; Published 27 June 2018

Academic Editor: Juan M. Coronado

The existence of H_2S has limited the biogas energy promotion. The traditional photodegradation of H_2S is usually conducted in the presence of O_2, yet this is unsuitable for biogas desulfurization which should be avoided. Therefore, the ultraviolet degradation of H_2S in the absence of O_2 was investigated for the first time in the present study from a mathematical point of view. Light wavelength and intensity applied were 185 nm and 2.16×10^{-12} Einstein/cm^2·s, respectively. Firstly, the mathematical model of H_2S photodegradation was established with MATLAB software, including the gas flow distribution model and radiation model of photoreactor, kinetics model, mass balance model, and calculation model of the degradation rate. Then, the influence of the initial H_2S concentration and gas retention time on the photodegradation rate were studied, for verification of the mathematical model. Results indicated that the photodegradation rate decreased with the increase in initial H_2S concentration, and the maximum photodegradation rate reached 62.8% under initial concentration of 3 mg/m^3. In addition, the photodegradation rate of H_2S increased with the increase in retention time. The experimental results were in good accordance with the modeling results, indicating the feasibility of the mathematical model to simulate the photodegradation of H_2S. Finally, the intermediate products were simulated and results showed that the main photodegradation products were found to be H_2 and elemental S, and concentrations of the two main products were close and agreed well with the reaction stoichiometric coefficients. Moreover, the concentration of free radicals of H• and SH• was rather low.

1. Introduction

During anaerobic digestion which is considered as one of the most important biomass-based renewable energy techniques to reclaim clean fuel of biogas [1], hydrogen sulfide (H_2S) is also produced in addition to CH_4 and CO_2, with content of 0.3%–0.4% [2]. H_2S is a foul acid gas, and it can result in the serious corrosion of pipeline, instruments, and equipment. In addition, H_2S endangers human health and causes environmental pollution. When the biogas containing H_2S is utilized as energy (such as burning, power generation, etc.), H_2S will be converted into SO_2 and cause serious air pollution [3]. Therefore, the existence of H_2S has limited the biogas energy promotion, and effective approaches are required for H_2S removal from biogas.

H_2S treatment methods include physical, chemical, biological, and combinatorial technologies. The direct degradation of H_2S for production of hydrogen and sulfur has been the research focus of domestic and foreign researchers, since it can effectively control the H_2S pollution produced during oil, gas, coal, and mineral processing and also achieve the recycling of hydrogen energy. The main methods of H_2S degradation for hydrogen and sulfur production include thermal degradation [4, 5], electrochemical degradation [6], photocatalytic degradation [7–9], and plasma degradation [10, 11]. Herein, photocatalytic degradation of H_2S is the most promising technology due to the high treatment efficiency and reaction rate.

Currently, researches on photocatalytic degradation of H_2S are mostly conducted under the condition of O_2 [12–14].

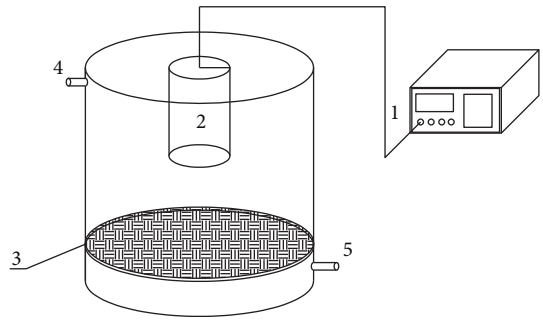

Figure 1: H_2S photodegradation reactor. (1) High-frequency generator, (2) electrodeless VUV lamp, (3) gas distribution device, (4) gas outlet, and (5) gas inlet.

Nevertheless, there is potential of explosion with O_2 presented during photocatalytic degradation of H_2S from biogas. Moreover, a by-product of ozone (O_3) is produced and further treatment was required. Photocatalytic degradation of H_2S with the absence of O_2 can avoid the abovementioned problems, which is quite suitable for H_2S removal from biogas and other gas treatments requiring anaerobic conditions. In addition, conventional UV light sources for degradation, such as mercury vapor lamps and high-pressure xenon lamps, are incapable of producing intense light near UV or deep UV lights. The self-made high-frequency discharge vacuum ultraviolet (VUV) lamp has lots of advantages compared with the conventional UV lamps and microwave discharge electrodeless lamps, such as high efficiency, high radiation intensity, high ratio of 185 nm light, and long service life [12, 15].

Therefore, in the present study, the photodegradation of H_2S with VUV lamp in the absence of O_2 was studied. Firstly, the photodegradation model was built using the MATLAB software, and then the effect of initial H_2S concentration and retention time on H_2S degradation performance was investigated and compared with the modeling result. Moreover, the reaction kinetics and mechanism of H_2S degradation in the absence of O_2 were discussed. We hope the research result can help the effective H_2S removal under anaerobic conditions.

2. Materials and Methods

2.1. Reactor and Experiments. Figure 1 schematically depicts the H_2S photodegradation reactor used in this study. The reactor was designed as cylindrical in shape to avoid the dead space for photodegradation and the potential uneven gas distribution within the reactor. A cylindrical VUV lamp was placed on top of the reactor, and its connection with the reactor was sealed with corrosion-resistant and high temperature-resistant silica gel. A high-frequency generator was connected with the VUV lamp via an external circuit. A porous plate-like gas distribution device was installed at the gas inlet, and thus, the incoming gas can evenly flow upwards. The gas outlet was installed at the top of the reactor. To avoid short flow, the gas inlet and outlet were placed on different sides of the reactor. For the sake of shielding the high-frequency electromagnetic radiation and preventing the corrosion of the reactor caused by H_2S, the body of the reactor was made of SUS304 stainless steel.

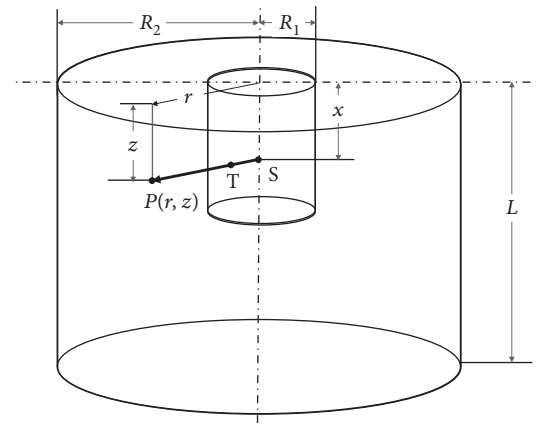

Figure 2: Cylindrical photoreactor with a cylindrical light source.

The diameter and height of the reactor were 15 and 14 cm, respectively. The total volume of the reactor was 2.5 L, with the effective volume of 2.0 L when the cylindrical UV lamp with a height of 5.8 cm and diameter of 4 cm was placed.

Figure 2 is diagrammatic sketch of the cylindrical photoreactor with a cylindrical light source for radiation field modeling, where $I(r, z)$ is the light intensity at point $P(r, z)$ within the reactor, $S_{L,\lambda}$ is the UV intensity at wavelength λ, and r and z are the horizontal distance and vertical distance of a random particle from the center of the UV lamp, respectively. L is the length of the UV lamp. μ_λ is the absorption coefficient of the medium in the reactor at the wavelength of λ. R_1 and R_2 are the radii of the cylindrical UV lamp and the cylindrical reactor, respectively.

2.2. Experimental Methods. In order to investigate the degradation efficiency of H_2S with only the high-frequency electrodeless VUV lamp without addition of O_3, OH, and photocatalyst, the reactor was firstly dried, and Ar was flushed into the reactor with a 10 L/min flow rate for an hour to expel the residual O_2 and H_2O in the pipeline. During the whole experiment, Ar gas was continuously flushed to exclude the effects of O_3 and OH on H_2S degradation.

2.3. Analytical Methods. H_2S concentration was determined with methylene blue spectrophotometry under a wavelength of 660 nm [16].

3. Results and Discussion

3.1. Mathematical Modeling of H_2S Photodegradation

3.1.1. Gas Flow Distribution Model. The rate of gas flow was determined by both the annular space of the reactor and the retention time. As the diameter of the reactor and the UV lamp were 15 cm and 4 cm, respectively, the rate of the gas flow was calculated as 20–40 L/min when the retention time was set as 3–6 s. Considering that the concentration of H_2S in the gas influent was low, the Re constant could be calculated based on the physical properties of the incoming

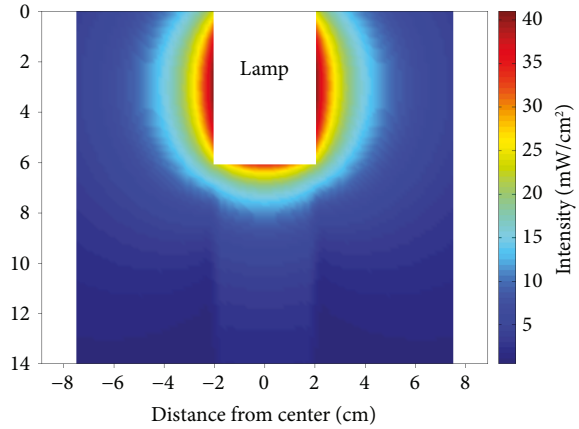

Figure 3: The light intensity distribution in the photoreactor.

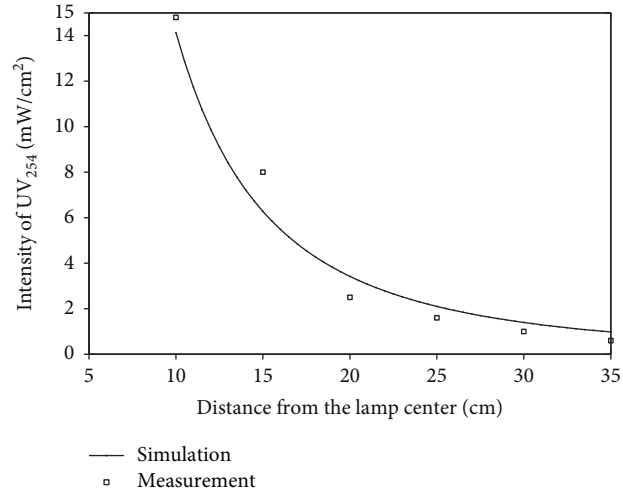

Figure 4: The experimental data and simulation data of the UV intensity with the change of space.

gas. The Re calculated at room temperature with Ar as carrier gas was 203–406.

The velocity (v) of a particle at the radius of R away from the center axis of the annular reactor can be determined according to the following equation [13]:

$$v = \frac{\left(2U\left(R_2^2 - R_1^2\right)/\ln R_2/R_1\right)\ln\left(R/R_1\right) - 2U\left(R^2 - R_1^2\right)}{R_1^2 + R_2^2 - \left(\left(R_2^2 - R_1^2\right)/\ln R_2/R_1\right)}, \quad (1)$$

where U is the known average velocity and R_1, R_2, and R are the radius of the UV lamp, the radius of the reactor, and the horizontal distance between the particle and the center axis of the annular reactor, respectively.

Based on (1), the simulated maximum velocity was no more than 5.8 m/s (as shown in Figure S1), and then the calculated Re was also no more than 609. The above Re values were all far below the critical value of laminar flow (2300) and indicated a typical laminar flow pattern in the reactor (the Re calculation was provided in the Supplementary Materials).

3.1.2. Radiation Field Model. The light intensity ($I(r,z)$) at point $P(r,z)$ within the reactor can be expressed with (2) [17].

$$I(r,z)_\lambda = \frac{S_{L,\lambda}}{\pi^2}\int_0^L \frac{r}{\left[r^2 + (z-x)^2\right]^{3/2}} \times \exp \cdot \left[-\mu_\lambda\left(r^2 + (z-x)^2\right)^{1/2}\left(1 - \frac{R_1}{r}\right)\right] dx. \quad (2)$$

The simulated three-dimensional model of the light intensity by the cylindrical VUV lamp at the center of the photoreactor with diameter and height of 15 cm and 14 cm, respectively, is shown in Figure 3. The white area was occupied by the VUV lamp with diameter and height of 4 cm and 5.8 cm, respectively, as scaled in the figure coordinate axis. According to Figure 3, light intensity decreased rapidly with the increase in the distance from the center of the light source.

In order to verify the result of the light intensity distribution model in the reactor, a UV radiation meter was applied to measure the UV_{254} intensity at 5–35 cm away from the lamp wick of the cylindrical lamp. In the meantime, the light intensity at the same position was calculated based on the UV light radiation field model and then was compared with the measured value to verify the results of the model. As shown in Figure 4, the results indicated that the calculated value and the measured values were close, indicating that (2) was feasible to predict the radiation intensity distribution.

3.1.3. Photochemical Reaction Kinetics Model. The photochemical reaction kinetics equation involving component i can generally be presented as the following equation.

$$\frac{dC_i}{dt} = \Phi_i \cdot I \cdot \left(1 - 10^{\varepsilon b C_i}\right), \quad (3)$$

where C_i is the molar concentration of component i (mol/L), Φ_i is the quantum efficiency, ε is the molar absorption coefficient (L/mol·cm), b is the optical length (cm), and I is the light radiation intensity (Einstein/cm^2·s). It should be noted that the VUV light absorption by other components of the initial biogas, including the typical CH_4 and CO_2, could be neglected [18].

Equation (3) has an exponential term, making the calculation complicated. When $\varepsilon b C_i < 0.02$, (3) can be reasonably approximated to the following expression:

$$\frac{dC_i}{dt} = 2.303 \cdot \Phi_i I \varepsilon b C_i. \quad (4)$$

Asili and De Visscher [13] proposed another equation for calculating the photochemical reaction rate r_i (molecule/cm^3·s):

$$-r_i = \Phi_i \cdot C_i \cdot \sigma_i \cdot E_p, \quad (5)$$

where C_i is the molar concentration of component i (molecule/cm^3), Φ_i is the quantum efficiency, σ_i is the absorption cross section of component i, and E_p is the photon flux (photon/cm^2·s).

The comparison of (4) and (5) revealed that both equations reflect the same reaction behavior, though (4) describes the concentration change macroscopically while (5) describes it microscopically. Both equations describe the chemical changes that occur when the reacting components absorb a certain amount of energy.

3.1.4. Mass Balance Model. Firstly, the Peclet number Pe in the photoreactor was calculated, revealing the numerical zone of 132–263. Pe represented the relative proportion of convection to diffusion. When Pe is larger than 40, the dominant mass transfer type was convection at the airflow direction. As the main gas flow pattern was a laminar flow, the main mass transfer pattern at the vertical direction was diffusion. According to the empirical equation, for H_2S-air mixed gas, the diffusion coefficient at the vertical direction can be expressed as [19]

$$D_{H_2S\text{-air}} = 0.7914T^{1.75}/\mathrm{P}, \tag{6}$$

where $D_{H_2S\text{-air}}$ is the diffusion coefficient (cm^2/s), T is the gas temperature (K), and P is the gas pressure.

For a random component i of the photochemical reaction system in the annular photoreactor, its partial differential equation of mass conservation can be represented as

$$v \cdot \frac{\partial C_i}{\partial L} = D_i \cdot \frac{\partial^2 C_i}{\partial R^2} + \frac{D_i}{R} \cdot \frac{\partial C_i}{\partial R} + r_i, \tag{7}$$

where v is the velocity of the gas molecule at current position (cm/s), C_i is the molar concentration of the component i ($mole/cm^3$), L is the vertical distance between a random position and the gas inlet (cm), R is the horizontal distance between a random position and the linear light source, D_i is the diffusion coefficient of the component i at the radical direction (cm^2/s), and r_i is the photochemical reaction rate ($mole/cm^3 \cdot s$).

The boundary condition of the partial differential equation (7) was assumed as the no-flow boundary, and the inlet gas concentration was considered as constant.

3.1.5. Calculation Model of Degradation Rate. For a random component i in the photochemical reaction system, the degradation degree η_i can be expressed as

$$\eta_i = 1 - \frac{\bar{C}_i}{C_{i,\text{initial}}}, \tag{8}$$

where $\bar{C}_i$ is the random component i in the photochemical reaction system at the gas outlet and $C_{i,\text{initial}}$ is the initial concentration of i at the inlet. For a tubular reactor, the average concentration of the random component i at the gas outlet can be expressed as

$$\bar{C}_i = \frac{\int_{R_1}^{R_2} v \cdot 2\pi R \cdot dR}{\int_{R_1}^{R_2} v \cdot 2\pi R \cdot dR}, \tag{9}$$

where v is the velocity of the gas molecule at the present position (cm/s), R_1 and R_2 are the radius of the VUV lamp and the reactor (cm), and R is the horizontal distance between a random position and the linear light source.

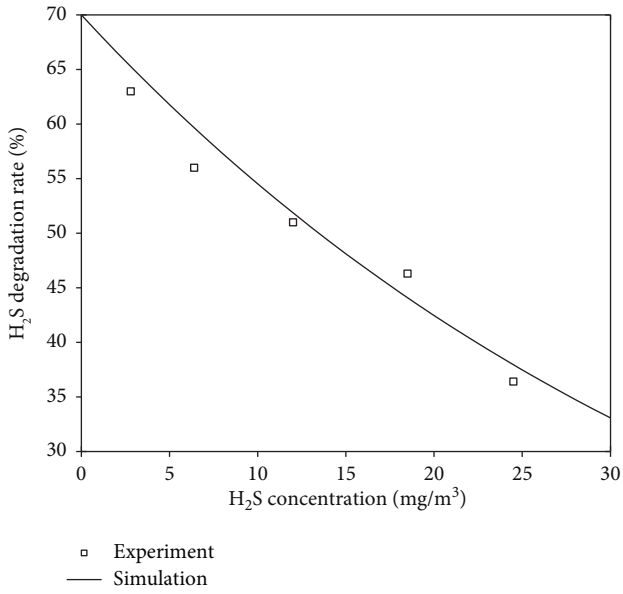

Figure 5: Influence of initial concentration of H_2S on the degradation rate.

The velocity of the component i in the reactor can be calculated using (1) and (2) and can be used to acquire the light intensity of a random position in the reactor. Then, the acquired data can be used in (4) and (7).

Equation (4) is an ordinary differential equation (ODE). Although (7) is a partial differential equation (PDE), it can be converted into a series of ODEs using MATLAB ODE15s for equation solution. Then, (8) and (9) are used for solving the degradation rate of the target component and correlate with experimental data.

3.2. Major Influence Factors on H_2S Photodegradation

3.2.1. Initial H_2S Concentration. The influence of the initial H_2S concentration on the degradation rate under retention time of 6 s is profiled in Figure 5. Results showed that the degradation rate continuously decreased with the increase in the initial H_2S concentration, which was similar to the situation with O_2 present [12]. As shown, when the initial H_2S concentration was 3 mg/m^3, the maximum degradation rate was about 62.8%. When the initial H_2S concentration reached 25 mg/m^3, the degradation rate decreased to 36.2%. UV light can only pass a relatively short distance in vacuum, and also there were no oxidative free radicals to assist degradation [20]; therefore, the degradation rate was comparatively lower than that with the presence of O_2 [12, 21]. Moreover, no SO_4^{2-} in the photodegradation products of H_2S was detected although it was confirmed as the main product in a previous study [22], and H_2 and elemental sulfur were the possible products. Yet, solid S was also not observable throughout the whole experiment. The first reason was the rather low particle settling velocity calculated by Stokes formula, and another reason was

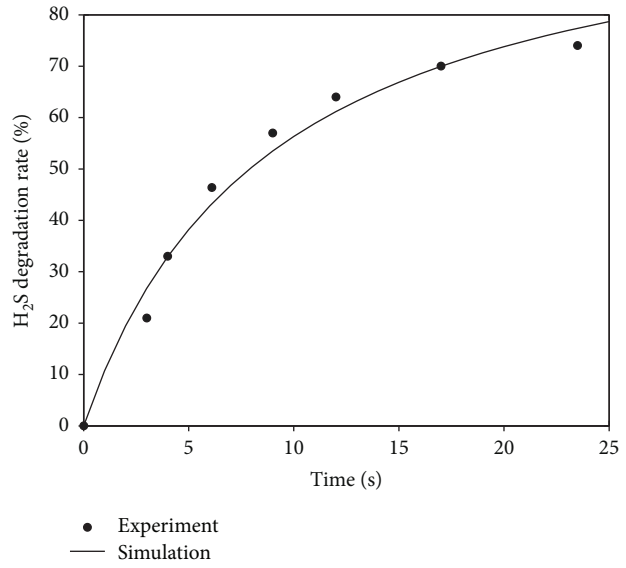

Figure 6: The relationship between H_2S degradation rate and retention time of direct photolysis by UV with the absence of oxygen.

the very low H_2S concentration and high airflow velocity. Therefore, it was difficult for the sulfur particle to settle on the internal reactor walls and no deposition of elemental sulfur was observed.

3.2.2. Gas Retention Time. Under the initial H_2S concentration of 12 mg/m^3, the simulation of the H_2S degradation profile based on modeling and the experimental data are compared in Figure 6. The experimental results indicated that the degradation rate was significantly affected when gas retention time in the reactor was less than 12 s. Specifically, when gas retention time was 3 s and 6 s, the degradation rate was 22.0% and 48.1%, respectively, indicating that the degradation efficiency proportionally increased with gas retention time. With higher gas retention time, the increasing rate of the degradation efficiency became slower. For instance, when gas retention time was 24 s, the degradation efficiency was 74% and only increased by 30% compared with that at gas retention time of 6 s. However, it still could not reach 100% degradation with the further increase in gas retention time.

The dead zone was placed in a position far away from the lamp, and so H_2S was hard to be degraded thoroughly. Longer retention time was beneficial for increasing the degradation rate; however, the energy consumption was also increased. Therefore, the appropriate retention time should be selected considering the initial H_2S concentration, equipment cost, and operating cost.

The root-mean-square error (RMSE) for this model simulation was as small as 0.0622. A t-test was conducted for comparing the simulation data and experimental data, and the test result accepted the null hypothesis with a possibility of 96.72%, indicating that the simulation data and the experimental data were consistent. This proves that the model to simulate the degradation efficiency in the photodegradation reactor was feasible.

3.3. Mechanism of H_2S Photodegradation Using Only VUV Light. Wilson et al. [23] studied the direct degradation of H_2S by photon of a near ultraviolet band. Results showed that a photon with a wavelength less than 270 nm could directly photodegrade H_2S into H· and SH·, and SH· could be degraded into H· and S· with a photon wavelength less than 230 nm, as shown in (10) and (11). The possible reactions during the direct photodegradation of H_2S are listed as follows:

$$H_2S + h\nu(\lambda \le 270\,\text{nm}) \rightarrow H\cdot + SH\cdot \quad (10)$$

$$HS\cdot + h\nu(\lambda \le 230\,\text{nm}) \rightarrow H\cdot + S \quad (11)$$

$$H\cdot + H_2S \rightarrow H_2 + HS\cdot \quad (12)$$

$$H\cdot + H\cdot \rightarrow H_2 \quad (13)$$

$$H\cdot + HS\cdot \rightarrow H_2 + S \quad (14)$$

$$HS\cdot + HS\cdot \rightarrow S + H_2S \quad (15)$$

By referring to the chemical dynamics database of the National Institute of Standards and Technology (NIST) and the related literatures, the rate constants can be acquired for the above reactions and are summarized in Table 1. A photon participates in reactions (10) and (11), and the molar absorption coefficients for wavelengths of 185 nm and 254 nm can be obtained by converting the absorptivity data summarized in Table 1.

Based on (10), (11), (12), (13), (14), and (15), the degradation rate equation of the various intermediates during hydrogen sulfide photodegradation in the absence of O_2 could be established. As photon is presented in (10) and (11), let $k_{obs} = 2.030\Phi_i \varepsilon b$ ((4)), denoting k_{obs1}, k_{obs2}, k_3, k_4, k_5, and k_6 as the rate constants for (10), (11), (12), (13), (14), and (15). The reaction rate equations for each component can be expressed as follows:

$$\frac{d[H_2S]}{dt} = -k_{obs1}\cdot[H_2S] - k_3\cdot[H_2S][H\cdot] + k_6\cdot[SH\cdot]^2, \quad (16)$$

$$\frac{d[H\cdot]}{dt} = k_{obs1}\cdot[H_2S] + k_{obs2}\cdot[SH\cdot] - k_3\cdot[H_2S][H\cdot] - k_4\cdot[H\cdot]^2 - k_5\cdot[SH\cdot][H\cdot], \quad (17)$$

$$\frac{d[SH\cdot]}{dt} = k_{obs1}\cdot[H_2S] - k_{obs2}\cdot[SH\cdot] - k_5\cdot[SH\cdot][H\cdot] - k_6\cdot[SH\cdot]^2, \quad (18)$$

$$\frac{d[H_2]}{dt} = k_3\cdot[H_2S][H\cdot] + k_4\cdot[H\cdot]^2 + k_5\cdot[H\cdot][SH\cdot], \quad (19)$$

$$\frac{d[S]}{dt} = k_{obs2}\cdot[SH\cdot] + k_5\cdot[SH\cdot][H\cdot] + k_6\cdot[SH\cdot]^2. \quad (20)$$

Then, the reaction rate equations for H_2S, H·, SH·, H_2, and S (from (16), (17), (18), (19), and (20)) were integrated into the UV-photodegrading reactor model, and the H_2S photodegradation effect without O_2 was simulated under the following conditions: the initial H_2S concentration was set as 12 mg/m^3 with Ar as the carrier gas. The concentration

Table 1: The chemical reaction of direct photolysis of H_2S and the corresponding photolysis rate constants.

Reaction	Quantum efficiency	Light absorptivity at 185 nm (L/mol·cm)	Light absorptivity at 254 nm (L/mol·cm)	Rate constant (L/mol·s)	Reaction order	References
$H_2S + h\nu \rightarrow H\cdot + SH$	1	1004.66	1.96	/	/	[24]
$HS\cdot + h\nu \rightarrow H\cdot + S$	1	20.5	0	/	/	[24]
$H\cdot + H\cdot \rightarrow H_2$	/	/	/	$2.498E+10$	2	[25]
$H_2S + H\cdot \rightarrow H_2 + SH$	/	/	/	$4.786E+08$	2	[26]
$H\cdot + SH\cdot \rightarrow H_2 + S$	/	/	/	$8.0E+09$	2	[27]
$SH\cdot + SH\cdot \rightarrow S + H_2S$	/	/	/	$8.368E+9$	2	[28]

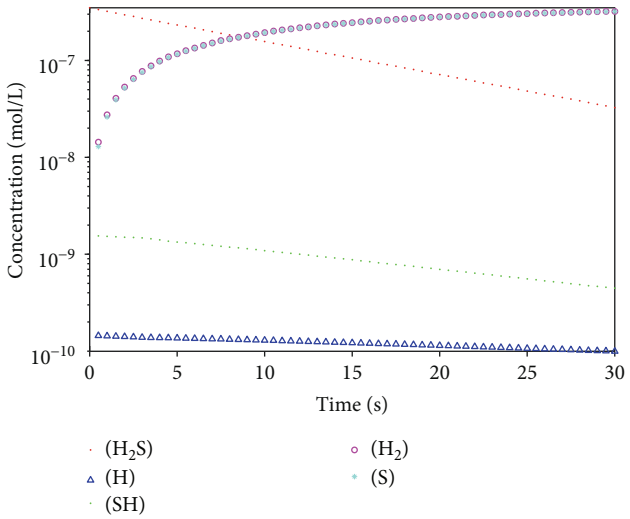

Figure 7: The simulated concentration changes of components of H_2S photodegradation by UV without the presence of oxygen.

evolution of H_2S, $H\cdot$, $SH\cdot$, H_2, and S were calculated 2 cm away from the UV light with MATLAB software and demonstrated by the logarithmic scale in Figure 7.

It was revealed that the final products of H_2S photodegradation were mainly H_2 and S, and their concentrations were close to each other, which was in accordance with the stoichiometric coefficients of the photodegradation reaction. Moreover, the simulated concentrations of $H\cdot$ and $SH\cdot$ radicals were rather low, which were about two orders of magnitude lower than H_2 and S.

Finally, we tried to build the analytical equation connecting the rate of H_2S consumption and its concentration and light intensity using steady-state approximation for radicals. Firstly, let (16) be equal to zero, as shown in (21).

$$\frac{d[H_2S]}{dt} = 0. \tag{21}$$

Then, (21) and (22) could be obtained combining (16) and (21), as follows.

$$[H_2S]_{s\text{-}t}(k_{obs1} + k_3[H\cdot]) = k_6[SH\cdot]^2, \tag{22}$$

$$[H_2S]_{s\text{-}t} = \frac{k_6[SH\cdot]^2}{k_{obs1} + k_3[H\cdot]}. \tag{23}$$

Then, k_{obs1} was substituted with (4), and the analytical equation connecting the rate of H_2S consumption and its concentration and light intensity using steady-state approximation for the radical could be obtained as (24).

$$[H_2S]_{s\text{-}t} = \frac{k_6[SH\cdot]^2}{2.303\cdot\Phi_i I\varepsilon b C_i + k_3[H\cdot]}. \tag{24}$$

4. Conclusions

In the present study, the mathematical model of ultraviolet degradation of H_2S with the absence of O_2 was established, and the influence of the initial H_2S concentration and gas retention time on the photodegradation rate were studied and for verification of the model. The main findings were as follows.

(1) The photodegradation rate decreased with the increase in initial H_2S concentration, and the maximum photodegradation rate was about 62.8% under initial concentration of 3 mg/m^3.

(2) The photodegradation rate increased with the increase in H_2S retention time.

(3) Experimental results were in good accordance with the modeling results.

(4) The main photodegradation products were H_2 and elemental S based on mathematical modeling. Concentrations of both products were close and agreed well with the reaction stoichiometric coefficients.

Data Availability

The data used to support the findings of this study are available from the corresponding author upon request.

Conflicts of Interest

The authors declare that they have no conflicts of interest.

Authors' Contributions

Jian-hui Xu and Bin-bin Ding contributed equally to this work and should be considered co-first authors.

Acknowledgments

The authors gratefully acknowledge the financial support of the Development of Social Science and Technology in Dongguan (Key) (2017507101426).

Supplementary Materials

Calculation of Reynolds number (Re): the calculation formula for Re was $\mathrm{Re} = \rho v d/\mu$, where ρ, v, and μ were the gas density (1.169 g/cm^3), velocity, and viscosity coefficient (18.448 μPa·s) of Ar gas, respectively, and d was the equivalent diameter of the photoreactor. The diameter (d) was 0.15 cm. The velocity (v) was 0.019–0.038 m/s based on the gas flow rate ($v = Q/S$, where Q was 20–40 L/min and S was obtained based on the diameter of 15 cm). Then the calculated Re was about 203–406. In addition, the velocity based on the simulation of (1) was no more than 0.058 m/s (as shown in Figure S1), and Re was about 609. Both the above Re values indicated a typical laminar flow pattern in the reactor. Figure S1: the simulated gas flow velocity by (1). *(Supplementary Materials)*

References

[1] G. Silvestre, B. Fernandez, and A. Bonmati, "Significance of anaerobic digestion as a source of clean energy in wastewater treatment plants," *Energy Conversion and Management*, vol. 101, pp. 255–262, 2015.

[2] A. M. Montebello, M. Mora, L. R. López et al., "Aerobic desulfurization of biogas by acidic biotrickling filtration in a randomly packed reactor," *Journal of Hazardous Materials*, vol. 280, pp. 200–208, 2014.

[3] X. Song, W. Yao, B. Zhang, and Y. Wu, "Application of Pt/CdS for the photocatalytic flue gas desulfurization," *International Journal of Photoenergy*, vol. 2012, Article ID 684735, 5 pages, 2012.

[4] N. O. Guldal, H. E. Figen, and S. Z. Baykara, "New catalysts for hydrogen production from H_2S: preliminary results," *International Journal of Hydrogen Energy*, vol. 40, no. 24, pp. 7452–7458, 2015.

[5] K. Akamatsu, M. Nakane, T. Sugawara, T. Hattori, and S. Nakao, "Development of a membrane reactor for decomposing hydrogen sulfide into hydrogen using a high-performance amorphous silica membrane," *Journal of Membrane Science*, vol. 325, no. 1, pp. 16–19, 2008.

[6] A. A. Anani, Z. Mao, R. E. White, S. Srinivasan, and A. J. Appleby, "Electrochemical production of hydrogen and sulfur by low-temperature decomposition of hydrogen sulfide in an aqueous alkaline solution," *Journal of the Electrochemical Society*, vol. 137, no. 9, pp. 2703–2709, 1990.

[7] X. Zong, J. Han, B. Seger et al., "An integrated photoelectrochemical–chemical loop for solar-driven overall splitting of hydrogen sulfide," *Angewandte Chemie*, vol. 53, no. 17, pp. 4399–4403, 2014.

[8] X. Bai, Y. Cao, and W. Wu, "Photocatalytic decomposition of H_2S to produce H_2 over CdS nanoparticles formed in HY-zeolite pore," *Renewable Energy*, vol. 36, no. 10, pp. 2589–2592, 2011.

[9] H. Yan, J. Yang, G. Ma et al., "Visible-light-driven hydrogen production with extremely high quantum efficiency on Pt–PdS/CdS photocatalyst," *Journal of Catalysis*, vol. 266, no. 2, pp. 165–168, 2009.

[10] E. Linga Reddy, J. Karuppiah, V. M. Biju, and C. Subrahmanyam, "Catalytic packed bed non-thermal plasma reactor for the extraction of hydrogen from hydrogen sulfide," *International Journal of Energy Research*, vol. 37, no. 11, pp. 1280–1286, 2013.

[11] S. John, J. C. Hamann, S. S. Muknahallipatna, S. Legowski, J. F. Ackerman, and M. D. Argyle, "Energy efficiency of hydrogen sulfide decomposition in a pulsed corona discharge reactor," *Chemical Engineering Science*, vol. 64, no. 23, pp. 4826–4834, 2009.

[12] J. Xu, C. Li, P. Liu, D. He, J. Wang, and Q. Zhang, "Photolysis of low concentration H_2S under UV/VUV irradiation emitted from high frequency discharge electrodeless lamps," *Chemosphere*, vol. 109, pp. 202–207, 2014.

[13] V. Asili and A. De Visscher, "Mechanistic model for ultraviolet degradation of H_2S and NO_x in waste gas," *Chemical Engineering Journal*, vol. 244, pp. 597–603, 2014.

[14] R. Portela, M. C. Canela, B. Sanchez et al., "H_2S photodegradation by TiO_2/M-MCM-41 (M = Cr or Ce): deactivation and by-product generation under UV-A and visible light," *Applied Catalysis B: Environmental*, vol. 84, no. 3-4, pp. 643–650, 2008.

[15] J. Xu, C. Li, Q. Zhang, D. He, P. Liu, and Y. Ren, "Destruction of toluene by the combination of high frequency discharge electrodeless lamp and manganese oxide-impregnated granular activated carbon catalyst," *International Journal of Photoenergy*, vol. 2014, Article ID 365862, 9 pages, 2014.

[16] J. C. C. Santos and M. Korn, "Exploiting sulphide generation and gas diffusion separation in a flow system for indirect sulphite determination in wines and fruit juices," *Microchimica Acta*, vol. 153, no. 1-2, pp. 87–94, 2006.

[17] T. Yokota and S. Suzuki, "Estimation of light absorption rate in a tank type photoreactor with multiple lamps inside," *Journal of Chemical Engineering of Japan*, vol. 28, no. 3, pp. 300–305, 1995.

[18] H. G. Baldovi, J. Albero, B. Ferrer, D. Mateo, M. Alvaro, and H. García, "Gas-phase photochemical overall H_2S splitting by UV light irradiation," *ChemSusChem*, vol. 10, no. 9, pp. 1996–2000, 2017.

[19] R. B. Bird, W. E. Stewart, and E. N. Lightfoot, *Transport Phenomena*, John Wiley & Sons, New York, NY, USA, 2002.

[20] Z. Li, H. Li'an, and Y. Linsong, "The experimental investigations of dielectric barrier discharge and pulse corona discharge in air cleaning," *Plasma Science and Technology*, vol. 5, no. 5, pp. 1961–1964, 2003.

[21] L. Huang, L. Xia, X. Ge, H. Jing, W. Dong, and H. Hou, "Removal of H_2S from gas stream using combined plasma photolysis technique at atmospheric pressure," *Chemosphere*, vol. 88, no. 2, pp. 229–234, 2012.

[22] M. C. Canela, R. M. Alberici, and W. F. Jardim, "Gas-phase destruction of H_2S using TiO_2/UV-VIS," *Journal of Photochemistry and Photobiology A: Chemistry*, vol. 112, no. 1, pp. 73–80, 1998.

[23] S. H. S. Wilson, J. D. Howe, and M. N. R. Ashfold, "On the near ultraviolet photodissociation of hydrogen sulphide," *Molecular Physics*, vol. 88, no. 3, pp. 841–858, 1996.

[24] S. P. Sander, A. JPD, J. R. Barker et al., *Chemical Kinetics and Photochemical Data for Use in Atmospheric Studies: Evaluation Number 17*, JPL Publication, 2011.

[25] J. N. Bradley, S. P. Trueman, D. A. Whytock, and T. A. Zaleski, "Electron spin resonance study of the reaction of hydrogen atoms with hydrogen sulphide," *Journal of the Chemical Society, Faraday Transactions 1: Physical Chemistry in Condensed Phases*, vol. 69, no. 0, pp. 416–425, 1973.

[26] J. Peng, X. Hu, and P. Marshall, "Experimental and ab initio investigations of the kinetics of the reaction of H atoms with H_2S," *The Journal of Physical Chemistry A*, vol. 103, no. 27, pp. 5307–5311, 1999.

[27] G. Loraine, W. Glaze, and W. Glaze, "Destruction of vapor phase halogenated methanes by means of ultraviolet photolysis," *Proceedings of the Industrial Waste Conference*, vol. 47, pp. 309–316, 1993.

[28] R. A. Stachnik and M. J. Molina, "Kinetics of the reactions of mercapto radicals with nitrogen dioxide and oxygen," *The Journal of Physical Chemistry*, vol. 91, no. 17, pp. 4603–4606, 1987.